The Astrophysical Journal, 723:1711–1717, 2010 November 10 doi:10.1088/0004-637X/723/2/1711

PRECURSORS OF SHORT GAMMA-RAY BURSTS

E. Troja[1], S. Rosswog[2], and N. Gehrels[1]
[1] NASA, Goddard Space Flight Center, Greenbelt, MD 20771, USA
[2] School of Engineering and Science, Jacobs University Bremen, Campus Ring 1, 28759 Bremen, Germany
Received 2010 June 7; accepted 2010 September 7; published 2010 October 26

ABSTRACT

We carried out a systematic search of precursors on the sample of short gamma-ray bursts (GRBs) observed by *Swift*. We found that ∼8%–10% of short GRBs display such early episodes of emission. One burst (GRB 090510) shows two precursor events, the former ∼13 s and the latter ∼0.5 s before the GRB. We did not find any substantial difference between the precursor and the main GRB emission, and between short GRBs with and without precursors. We discuss possible mechanisms to reproduce the observed precursor emission within the scenario of compact object mergers. The implications of our results on quantum gravity constraints are also discussed.

Key words: gamma-ray burst: general – gamma-ray burst: individual (GRB090510) – stars: neutron

Online-only material: color figures

1. INTRODUCTION

The main gamma-ray event in gamma-ray bursts (GRBs) is occasionally anticipated by a less-intense episode of emission, called a precursor. With the exception of a few cases, precursors show non-thermal spectra and have been mainly observed in long duration GRBs (e.g., Lazzati 2005; Burlon et al. 2008). The first evidence of preburst activity has been observed by the *Ginga* satellite in the long GRB 900126 (Murakami et al. 1991), where a soft X-ray peak precedes the burst onset by ∼8 s. This is one of the few examples of a precursor with a thermal spectrum.

Observationally, the identification of a precursor is highly dependent on its operational definition and might further suffer from instrumental biases. A first systematic search of precursors (Koshut et al. 1995) showed that only 3% of GRBs observed by BATSE exhibit a precursor event, having no substantially different properties with respect to the γ-ray prompt emission. By using a different search criterion, Lazzati (2005) found instead that ∼20% of long GRBs are preceded by an early emission episode, which is much weaker and spectrally softer than the proper GRB. This result was also confirmed by *BeppoSAX* (Piro et al. 2005) and *HETE-2* (Vanderspek et al. 2004) observations, yet it is unclear whether it still holds for the precursor activity detected in *Swift* GRBs. Hints of different properties (e.g., hardness ratio (HR), spectral lag) between the precursor and the prompt emission have been reported in the study of single bursts (e.g., GRB061121; Page et al. 2007). However the recent work of Burlon et al. (2008), based on a large sample of long GRBs observed by *Swift*, did not find evidence for such spectral distinction.

A ubiquitous feature, emerging from all the previous studies, is the distribution of delay times between the precursor and the prompt emission, which extends up to hundreds of seconds. This represents one of the main challenges to the current theoretical models. If the precursor marks the start of the central engine activity (Nakamura 2000), the observed quiescent time would require a fine tuning of the ejecta Lorentz factors or an effective turnoff of the GRB energy source (Ramirez-Ruiz et al. 2001). However, whether this early emission physically differs from the burst itself or is part of the same event remains a controversial point. Precursors as a separate phenomenon have also been discussed in several theoretical scenarios (e.g., Lyutikov & Usov 2000; Mészáros et al. 2001; Waxman & Mészáros 2003; Lyutikov & Blandford 2003; Umeda et al. 2005; Wang & Mészáros 2007). A set of models explains the precursor emission within the standard fireball scenario, commonly invoked to interpret the prompt and afterglow emission of GRBs. Within this framework the precursor is associated with the transition of the fireball to the optically thin regime, which produces a photospheric blackbody emission (Paczynski 1986; Mészáros et al. 2001; Daigne & Mochkovitch 2002; Ruffini et al. 2008), while the GRB is associated with the later formation of shocks at larger radii (Rees & Meszaros 1994). According to this interpretation, precursors happen relatively close in time to the GRB and should be observable in both long and short bursts.

Another class of models interprets the precursor within the collapsar scenario and links its origin to the jet break-out from the stellar surface (e.g., Ramirez-Ruiz et al. 2002; Waxman & Mészáros 2003; Zhang et al. 2003; Lazzati & Begelman 2005). The temporal delay between the precursor and the GRB is explained as an apparent period of quiescence due to viewing angle effects (e.g., Morsony et al. 2007) or, alternatively, as an intrinsic property of the central engine, which might undergo a second collapse (Wang & Mészáros 2007). In this case, precursors might be observed tens of seconds before the GRB emission and should occur exclusively in long GRBs. Indeed most of the observational and theoretical effort so far has been focused on long duration GRBs.

Little attention has been paid to the occurrence of precursors in short GRBs, and the possibility of an early precursor emission originated in the last moments of a compact binary merger has been sporadically discussed in the literature (e.g., Hansen & Lyutikov 2001; Rosswog & Ramirez-Ruiz 2002). In this paper, we explore in detail the observational evidence for precursors in short GRBs and discuss the implications. The paper is organized as follows. In Section 2, we describe the selection criteria and the detection method adopted to identify the precursor emission; the resulting sample of precursors and their properties is presented in Section 3; in Section 4, we discuss our findings in the framework of fireball and progenitor precursors (Section 4.1). In Section 4.2, we focus on the precursor emission observed in GRB 090510 and the implications for quantum gravity constraints.

2. DATA ANALYSIS

Up to 2010 January *Swift* detected 38 GRBs classified as short bursts ($T_{90} \lesssim 2$ s). We included in our sample 11 additional GRBs, which belong to the so-called group of short bursts with extended emission (EE; Norris & Bonnell 2006). As the classification of these bursts is unclear (Bloom et al. 2008; Zhang et al. 2009), we considered them as a separate group.

We searched the selected sample of 49 *Swift*/Burst Alert Telescope (BAT) GRBs for signal preceding the main gamma-ray event. We define precursors as those events which fulfill the following requirements: (1) the peak flux is smaller than the main event, (2) the flux returns to the background level before the start of the main event, and (3) the event location in the sky corresponds to the GRB position.

The *Swift* data were retrieved from the public archive[3] and processed with the standard *Swift* analysis software (v3.5) included in the NASA's HEASARC software (HEASOFT, ver. 6.8) and the relevant calibration files. Our analysis has been performed in the 15–150 keV energy band.

2.1. Temporal Analysis

As a first step, we inspected the GRB temporal profiles searching for precursor events, as defined in (1) and (2). For each GRB in the sample we created a light curve with a time bin of 0.128 ms, as shorter timescales are subject to noise fluctuations. In the case of *Swift*/BAT on-board triggers ∼300 s of event data are usually collected before the GRB trigger. We excluded from our analysis those time intervals during which the spacecraft was slewing, starting our search on average ∼240 s before the GRB. In order to identify the presence of weak emission in the GRB light curves, we used a detection algorithm based on wavelet transforms (Torrence & Compo 1998) with a Morlet mother function. The wavelet algorithm performs a multi scale analysis which is well suited for detecting a transient event, such as a precursor, whose duration is a priori unknown. We sampled 13 different timescales with a base-two logarithmic spacing, where the smallest resolvable scale s_0 is set by the light curve temporal resolution δt ($s_0 = 2\delta t$) and the maximum scale was arbitrarily set to 4 s.

As the count rates derived from mask-weighting procedures are already background subtracted, the preburst light curves are dominated by a white Gaussian noise due to statistical fluctuations (Rizzuto et al. 2007). In this particular case, the wavelet coefficients are normally distributed (Lazzati et al. 1999) and their power spectra follow a chi-square distribution with two degrees of freedom. Because of this property the significance levels of each peak in the wavelet power spectrum can be analytically derived (see, e.g., Torrence & Compo 1998). We examined the global wavelet spectrum, i.e., the time average over all the local wavelet spectra, for peak exceeding the noise spectrum level and set a minimum threshold of 99.7% significance (corresponding to a 3σ for a two-sided Gaussian distribution). In three cases (GRB 070406, GRB 080121, and GRB 091117) out of 49, the burst has been discovered in ground analysis and only ∼10 s of event data around the trigger time are available. Our search has therefore been restricted to that interval. Because of border effects due to the very short time interval, we did not apply the wavelet detection method and the light curves of these three bursts were simply inspected by eye.

We found that 4 out of 38 short bursts and 1 out of 11 bursts with EE show a possible precursor activity. Among them, one burst (GRB 090510) shows two precursor events, the former ∼13 s and the latter, already known in the literature (Abdo et al. 2009), ∼0.5 s before the GRB. The mask-weighted light curves of these GRBs are shown in Figure 1. The vertical dashed lines in each panel mark the time interval of the candidate precursors.

With the selected threshold of significance (99.7%) we expect a number of 0.04 spurious detections in each light curve, as we sampled 13 different timescales, and a total of ∼2 spurious detections in the whole sample. Furthermore, we recall that the light curves derived using the mask-weighting technique are correct if there are no other bright sources in the BAT field of view. While this assumption usually holds during the main GRB, when the source is weak, such as in the case of precursor events, the contamination of nearby sources becomes significant and might therefore lead to spurious detections. Further analysis is therefore mandatory in order to verify if the features revealed by the wavelet algorithm are real and associated with the GRB.

We proceeded by checking whether the five selected GRBs were detected by other satellites and, if so, whether there was evidence of emission simultaneously with the BAT candidate precursor. Three GRBs (GRB 081024A, GRB 090510, and GRB 09117) have this requisite and in Figure 1 we compare their *Swift*/BAT light curves (reported in each upper panel) with the *Fermi*/GBM (GRB 090510 and GRB 081024A) and *Suzaku*/WAM (GRB 091117) light curves (reported in the bottom panel). Times are always given relative to the BAT trigger time. The cross-check of the light curves shows that the precursors in GRB 081024A and GRB 091117 can be confidently considered real, as a simultaneous episode of emission has been observed by *Fermi*/GBM and *Suzaku* respectively. Instead no significant emission above the background level is observed in correspondence of the first precursor at T_0-13 s in GRB 090510, while the second precursor at $T_0-0.5$ s is clearly detected by the *Fermi*/GBM. GRB 090510 also triggered *Suzaku* and Konus−Wind, unfortunately no time-resolved events are available during the interval of the first precursor at T_0-13 s and any short timescale variability is hard to detect. Indeed, *Suzaku* and Konus−Wind light curves (with a resolution of 1 s and 2.9 s, respectively) do not show any significant excess at such early times (K. Yamaoka & V. Pal'shin 2010, private communication). This non-detection does not necessarily imply that the feature is spurious. Possible explanations are the smaller effective areas compared to BAT, or a precursor with a soft spectrum, e.g., peaking in the BAT energy range, as also expected on theoretical grounds.

2.2. Imaging Analysis

In order to further check whether the excess in the light curve is related to the GRB, we produced a background-subtracted sky image in the interval of the candidate precursor and searched for a source at the GRB position. This step allows a better characterization of the background level, as the contribution of other nearby sources is properly removed. Results are reported in Table 1, which lists the GRB name, the precursor time interval, and the significance of the source in the image domain as calculated by the tool `batcelldetect`. If the precursor has been detected by other instruments (see Section 2.1), they are listed in the last column.

For a blind source detection a significance threshold of 6.5σ is usually adopted to confidently assess that a source is real. Indeed, the subthreshold experiment[4] carried out by the *Swift* team showed that lowering this threshold significantly increases

[3] http://heasarc.gsfc.nasa.gov/docs/swift/archive/

[4] http://gcn.gsfc.nasa.gov/subthreshold.html

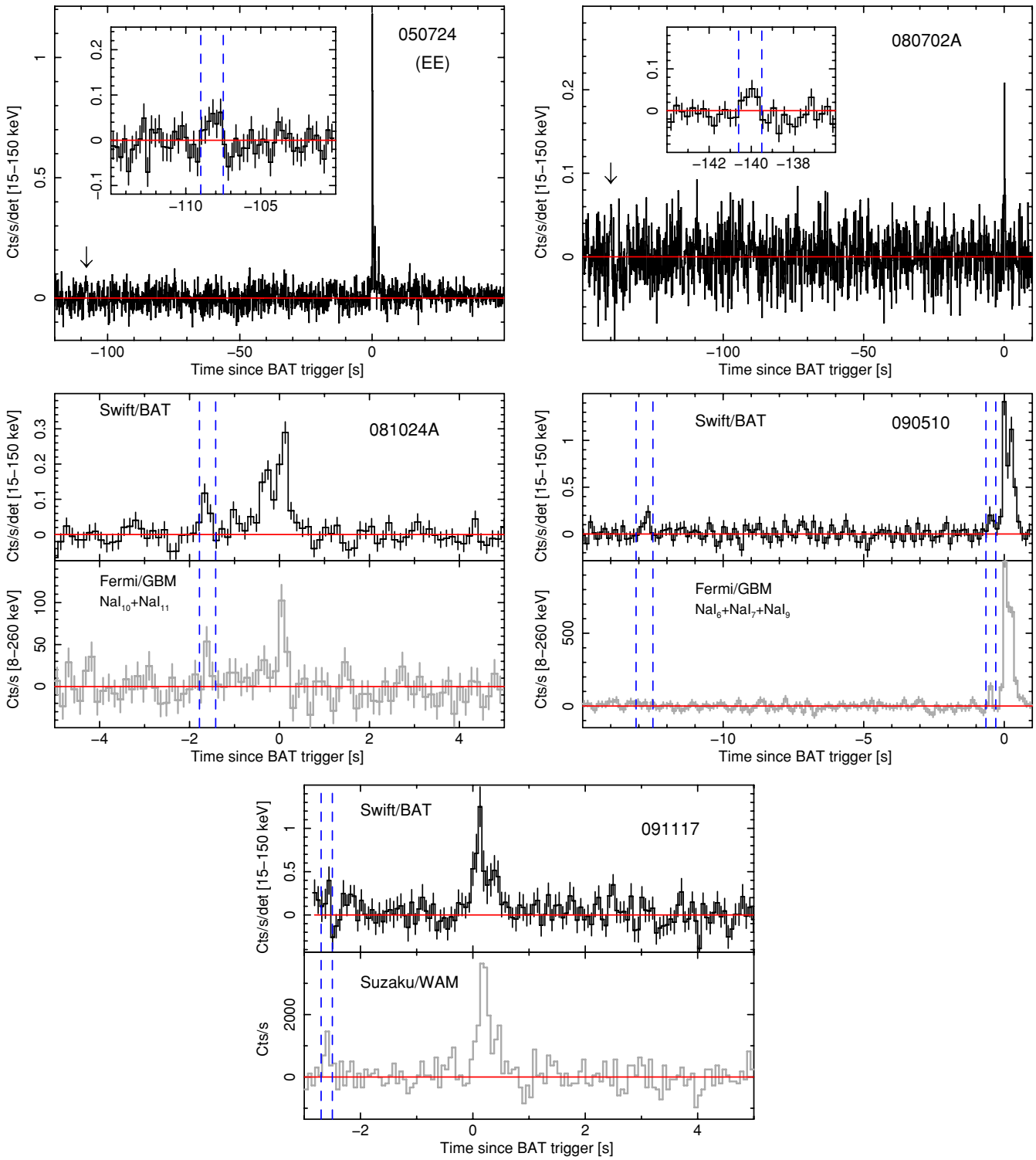

Figure 1. *Swift*/BAT mask-weighted light curves (15–150 keV) of short GRBs with a possible precursor activity. Dashed vertical lines mark the precursor duration. The precursors of GRB080702A and GRB050724 are shown in greater detail in the insets. For comparison, we also show the background-subtracted light curves of *Fermi*/GBM (090510 and 081024A) and *Suzaku*/WAM (091117).

(A color version of this figure is available in the online journal.)

the number of false detections (∼96% of false positives). However, our search was not performed on the whole image, as the source position was a priori known. This reduces the number of trials by a factor of $\sim 3 \times 10^4$, i.e., the number of independent pixels in a BAT image, with respect to a blind search and the 6.5σ threshold poses therefore a too restrictive cut.

We determined the probability to have a spurious $N\sigma$ detection at a fixed position through Monte Carlo simulations. An inspection of the detector plane images (DPIs) shows no noisy detectors during the selected time intervals, and therefore statistical fluctuations are the dominant source of noise. By assuming a Poissonian distribution with a mean count rate of ~ 0.12 counts s^{-1} det^{-1}, we simulated 10^5 source-free DPIs and

Table 1
Image Significance of the Candidate Precursors

GRB	T_i (s)	T_f (s)	Significance (σ)	Probability[a]	Others
050724 (EE)...	−108.5	−107.5	3.7	5×10^{-4}	...
080702A...	−140.6	−139.5	3.2	3×10^{-3}	...
081024A...	−1.70	−1.45	5.5	$<10^{-5}$	*Fermi*
090510 ...	−13.0	−12.6	5.2	$<10^{-5}$	...
	−0.55	−0.5	4.6	10^{-5}	*Fermi*
091117...	−2.75	−2.65	1.8	6×10^{-2}	*Suzaku*

Notes. [a] Probability of a spurious detection with equal or higher significance. Derived from Monte Carlo simulations.

derived the corresponding sky images. On each simulated image we ran the tool `batcelldetect` searching for a source at the GRB position. The probability that the detected source is due to background fluctuations is then calculated as the ratio between the total number of fictitious detections with significance equal or greater than that of the precursor (Table 1, Column 4) and the number of simulated images. The resulting values are listed in Table 1 (Column 5).

3. RESULTS

The results of our analysis are summarized in Table 1. We found evidence of a possible precursor activity in four short GRBs, out of a sample of 38 events, and in only one GRB with extended emission, out of a sample of 11 events. One burst (GRB 090510) shows two precursors, at $\sim T_0-13$ s and $\sim T_0-0.5$ s, respectively. The γ-ray light curves of these bursts have been shown in Figure 1. Our definition of precursor, detailed in Section 2, differs from those given in previous systematic studies (e.g., Koshut et al. 1995; Lazzati 2005), as it does not impose any particular constraint on the quiescence time or the instrumental trigger (e.g., Burlon et al. 2008). In only one case the classification of the event as a precursor depends on our operational definition: the latter precursor in GRB 090510 does not satisfy the conditions of either Koshut et al. (1995), because of its short delay time from the main GRB, or of Lazzati (2005), as the precursor event triggered the *Fermi*/GBM.

Because our wavelet analysis (Section 2.1) has been carried out on a large sample of events (46 GRB light curves) and probed various timescales (13, from 256 ms to 4 s) in each light curve, we expect the resulting sample of precursors to be contaminated by ∼2 spurious detections. A cross-check between *Swift* and other satellites confirms that at least three of our candidate precursors are real (Table 1, Column 5), namely, the cases of GRB 081024A, GRB090510 (second precursor), and GRB 091117.

We verified that the detected excess in the light curve corresponds to a point source at the GRB position in the image domain (Section 2.2; Table 1, Columns 3 and 4). The former precursor in GRB 090510 is detected at a $>5\sigma$ significance. Monte Carlo simulations showed that the probability of being a background fluctuation is very low ($<10^{-5}$), in agreement with the high significance of the detection. Two cases remain controversial. The precursors in GRB 080702A and GRB 050724 are detected at a significance of 3.2σ and 3.7σ, respectively, having a $\approx 10^{-3}$ probability of being spurious. They also have not been seen by other instruments. These two precursors are very intriguing, as they show the longest delay times from the GRB triggers ($\gtrsim$100 s) similar to those observed in some long GRBs. However, in the present study we are unable to confidently determine whether they are real features or not. In this context, it is worth noting that the only short GRB (BATSE trigger 2614) in the sample of Koshut et al. (1995) shows a precursor ∼75 s before the main burst. This strengthens the idea that long delay times are possible in short GRB precursors, as we will discuss in Section 4.1.2. Burlon et al. (2009) similarly proposed that a few short GRBs in the BATSE sample are preceded by precursors, sometimes with very long delays. A cross-check between the results of Burlon et al. (2009) and the BATSE 4B Catalogue (Paciesas et al. 1999) shows several incongruences. In particular, the durations quoted in the BATSE Catalogue are greater than 5 s.

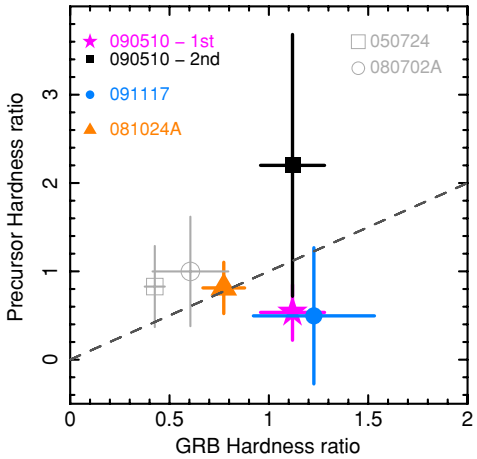

Figure 2. Hardness ratio of the precursor vs. hardness ratio of the main GRB event. Error bars are at 1σ confidence level. The dashed line shows where the two ratios are equal. The hardness ratio is defined as the count rate in the 50–150 keV band over the count rate in the 15–50 keV band. We also report the precursors of GRB 050724 and GRB 080702A, albeit we are unable to confidently determine whether they are real features, as explained in the text.
(A color version of this figure is available in the online journal.)

As our precursors are too faint to characterize their spectral shape, we investigated the presence of a possible spectral difference by comparing the precursor HR to that of the main GRB event. This is shown in Figure 2: all the precursors appear consistent with the main GRB properties, in agreement with the findings of Burlon et al. (2008). This result however might be partially a consequence of the *Swift*/BAT narrow bandpass. For instance, the broadband *Fermi* light curves of GRB 090510 (see Abdo et al. 2009; Figure 1) clearly shows that the main GRB event has an extremely hard spectrum, peaking in the MeV range, while the precursor at $T_0-0.5$ s peaks at around 200–300 keV. The precursor at T_0-13 s, found in the *Swift*/BAT light curves, is even softer, peaking in the 15–50 keV energy band (Figure 2, star symbol). On the other side, most theoretical models predict the peak of the precursor emission in the X-ray energy range, i.e., at the lower end of the BAT energy threshold. Therefore, independently of the BAT bandpass, this should be reflected in our Figure 2 by precursors occupying the region with HR $\lesssim 1$. Indeed, the points seem to follow this trend.

We further investigated whether short GRBs with precursors differ from the other short GRBs in the sample, either in the prompt or afterglow emission. We compared the distributions of their observed properties, such as γ-ray fluence, duration (T_{90}) and afterglow brightness, and ran a Kolmogorov–Smirnov (K-S) test between the two samples (short bursts with and without precursors). The probability that they belong to the same GRB population is 36%, based on the distribution of

their fluences (in the 15–150 keV band), and 34%, based on the distribution of their durations. Similarly a comparison of the X-ray (0.3–10 keV) afterglow flux distributions, observed at 100 s and 1000 s, shows no substantial difference (K-S test probability of 96% and 68%, respectively).

4. DISCUSSION

Precursor activity so far has been associated with long GRBs. Previous systematic studies have in fact been focused on the class of long GRBs, such as in the case of Lazzati (2005) who excluded those bursts with a duration $T_{90} \leqslant 5$ s, or biased against the detection of short duration precursors by the low time resolution, such as in the case of Koshut et al. (1995). This has led to the common notion that precursors are not present in short GRBs. For instance, McBreen et al. (2008) pointed out the presence of a precursor at T_0-8 s in the SN-less burst GRB 060505, considering this as a further dissimilarity with the class of short GRBs. Our analysis showed instead that short GRBs are also preceded by a precursor event, though less frequently than long GRBs (10% versus 20% of long GRBs). The precursors in our sample are characterized by short durations, never exceeding the GRB T_{90}. This disfavors the sub-jets model of Nakamura (2000), according to which the precursor duration is longer than that of the main burst.

Only one burst with extended emission (GRB 050724) shows a possible precursor ∼100 s before the onset of the main GRB. However, as discussed in Section 3, we cannot confirm in the present study whether it is a real event and therefore whether precursors are also present in bursts with EE. It has been suggested that bursts with EE may be originated by a different progenitor system (Troja et al. 2008; Metzger et al. 2008). The current sample of short bursts with EE is still too small to draw any conclusion, but the absence of precursors in this subset of bursts, if confirmed by future observations, could provide a further evidence of their different nature.

The association between precursors and long GRBs has also driven most of the theoretical work, which has often related the precursor to the interaction of the jet with the massive star progenitor (e.g., Ramirez-Ruiz et al. 2002; Lazzati & Begelman 2005). The presence of precursors in both long and short GRBs might represent a challenge for such interpretation. Given the fact that in the internal shock model (Rees & Meszaros 1994; Piran 1999) the GRB production is rather decoupled from the details of the central engine and both short and long bursts exhibit precursors, one may speculate that the precursor production is related to the fireball rather than the central engine itself. An obvious idea to test is whether the precursor could be caused by a fireball becoming optically thin (e.g., Goodman 1986) prior to the production of the prompt GRB emission. If we consider an "isolated" fireball (i.e., on becoming transparent the photons are not released into a surrounding, possibly intransparent environment), an observed duration of the precursor Δt would imply a fireball radius (at this stage) of $R \sim 2\Gamma^2 c\Delta t$, where Γ is the fireball bulk Lorentz factor. If we assume a saturated fireball with $\Gamma \approx \eta \equiv E/Mc^2$, where E is the fireball energy and M its baryonic mass loading, and equate the above radius to the one where the fireball should become transparent to its own photons (Abramowicz et al. 1991; Piran 1999), we find a relation between Γ and E for an observed duration Δt:

$$\Gamma \approx 25\ E_{51}^{1/5} \left(\frac{1\ \mathrm{s}}{\Delta t}\right)^{2/5}. \quad (1)$$

If, as indicated by recent *Fermi* results (Ackermann et al. 2010), short GRBs do indeed possess Lorentz factors in excess of 10^2, a precursor origin related to a fireball becoming optically thin would require a large fireball energy, $E > 10^{53}$ erg.

Moreover, if we assume that the main GRB signal is produced by internal shocks, then the variability timescale $\delta t_{\rm var}$ can be restricted to $\delta t_{\rm var} \gtrsim \Delta T$ (Lazzati 2005), where ΔT is the time interval between the precursor and the main prompt emission. The observed delays would suggest implausibly long variability timescales, longer than the main GRB duration itself. Thus, at least if the prompt emission is caused by internal shocks, we consider it unlikely that the observed precursors are produced by fireballs becoming optically thin. This conclusion could need to be modified if the fireball is released into an optically thick surrounding, say from a previously ejected wind (see Section 4.1.3).

4.1. Central Engine-related Mechanisms

Mergers of compact binaries, either in the form of a double neutron star (Blinnikov et al. 1984; Paczynski 1986; Goodman 1986; Eichler et al. 1989) or a neutron star–black hole system (Paczynski 1991; Narayan et al. 1992), are still arguably the most likely central engines of short GRBs. In the following we will focus on how such systems may produce an electromagnetic transient prior to the main GRB.

4.1.1. Interaction of Neutron Star Magnetospheres

Hansen & Lyutikov (2001) model the electromagnetic signatures that result from the interaction of two neutron star magnetospheres prior to a double neutron star merger. The main prediction of their model is an X-ray transient preceding the merger on a timescale of a few seconds. This signal could also be accompanied by a radio pulse.

Hansen & Lyutikov (2001) consider a binary system consisting of an old, recycled pulsar that is rapidly spinning ($P \approx$ 1–100 ms) and possesses a magnetic field of moderate strength ($B \sim 10^9$–10^{11} G) and a younger, slowly rotating ($P \approx$ 10–1000 s) strong-field ($B \sim 10^{12}$–10^{15} G) neutron star (possibly a magnetar), a combination that can be expected on evolutionary grounds. If the magnetar birth rate is about 10% of the "ordinary pulsar" birth rate, a decent fraction of double neutron stars should contain magnetars, at least initially. The recycled pulsar is considered as a perfectly conducting sphere that passes through the external field prescribed by the magnetar. In this way a dipolar magnetic field is induced whose magnetic dipole is directed against the external magnetic field. The motion of the pulsar through the external field induces surface charges that in turn produce electric fields with a component along the total magnetic field which accelerate charges in an attempt to short out this parallel electric field component. Once energetic enough, the latter produces curvature photons together with a dense population of electron–positron pairs. Pair plasma released into regions of increasing magnetic field strength are likely to be trapped in a optically thick cloud, while those released into regions of decreasing field strength result in a relativistically expanding wind of pairs and photons.

The strongest prediction of this model is the presence of an early precursor produced by the relativistic wind. The precursor spectrum should be close to thermal and hardening as the stars are driven toward coalescence. Interestingly, GRB 090510 has two precursor signals, where the first one peaks in the 15–50 keV energy band while the second peaks around 300 keV. Such behavior would be consistent with the predictions of the

Hansen–Lyutikov model. The maximum luminosity that the precursor can reach is of the order of

$$L \approx 7 \times 10^{45}\,\mathrm{erg\,s^{-1}} \left(\frac{B}{10^{15}\,\mathrm{G}}\right)^2 \left(\frac{a}{10^7\,\mathrm{cm}}\right)^{-7}. \quad (2)$$

It follows that in order to match with the observed properties of short GRB precursors a neutron star with a magnetar-like field ($B > 10^{15}$ G) is required. Such strong magnetic fields likely decay on much shorter timescales ($\sim 10^4$–10^5 yr; Heyl & Kulkarni 1998; Harding & Lai 2006, and references therein) than the merger lifetime, and a neutron star with a moderate magnetic field $B \sim 10^{12}$–10^{13} G looks a more plausible configuration. Some population synthesis models (Belczynski et al. 2002, 2006) however predict that a sizable fraction of double neutron star mergers has much shorter inspiral times. This short-lived channel peaks at an inspiral time of $\sim 3 \times 10^5$ years and after this time the magnetic field should have decayed by only a factor of a few (see Figure 1 of Heyl & Kulkarni 1998).

4.1.2. Neutron Star Flares Induced by Tidal Crust cracking

As a compact binary system secularly spirals in, the neutron star(s) become(s) vulnerable to tidal distortion. At a separation a the companion induces an ellipticity of $\epsilon_1 \sim \delta R_1/R_1 \sim \frac{m_2}{m_1}\left(\frac{R_{\rm ns}}{a}\right)^3$, where m_1 and m_2 are the neutron star masses and $R_{\rm ns}$ is the neutron star radius. Once the ellipticity exceeds a critical value, the neutron star crust cracks and likely triggers a violent restructuring of the magnetic field that may go along with a reconnection flare, similar to what is thought to happen in a magnetar giant flare (Thompson & Duncan 1995; Palmer et al. 2005; Hurley et al. 2005). Once the crust has been cracked for the first time, the neutron star enters a "tidal grinding phase" in which the tides exert a constant restructuring of crust, likely going along with further magnetic field reconfiguration and dissipation.

The exact numerical value of the critical ellipticity that the crust can still sustain, $\epsilon_{\rm c}$, is not well known, but recent studies based on molecular dynamics simulations (Horowitz & Kadau 2009) suggest that neutron star crusts can sustain strains up to a breaking value of $\sigma_{\rm max} \approx 0.1$, corresponding to critical ellipticities up to $\epsilon_{\rm c} \approx 4 \times 10^{-6}$ (Ushomirsky et al. 2000; Owen 2005). Thus, the tidally induced crust cracking is expected to occur at a separation of

$$a_{\rm crit} \approx 100 \left(\frac{m_2}{m_1}\right)^{1/3} \epsilon_{\rm c,-6}^{-1/3} R_{\rm ns}, \quad (3)$$

where $\epsilon_{\rm c,-6}^{-1/3}$ is the ellipticity in units of 10^{-6}. Applying the point-mass limit for a circular binary system (ignoring the effects of the finite stellar radii; Peters 1964) one finds for the duration of the tidal grinding phase prior to the merger:

$$\tau_{\rm tg} \approx \frac{5}{256}\frac{c^5}{G^3}\frac{a_{\rm crit}^4}{m_1 m_2 (m_1+m_2)} \approx 62\ \mathrm{min}\ \epsilon_{\rm c,-6}^{-4/3}\frac{2q^{1/3}}{1+q}\left(\frac{m_{\rm ns}}{1.4\,M_\odot}\right)^{-3}\left(\frac{R_{\rm ns}}{10\,\mathrm{km}}\right)^4, \quad (4)$$

where we defined the mass ratio $q = m_2/m_1$. Thus, for a binary system with the most likely parameters one expects the crust restructuring to set in about an hour ahead of the burst (where we have assumed that the delay between coalescence and burst is negligible). Should the crust be able to sustain substantially larger deformations, say an order of magnitude more, this duration could be brought down to minutes. Due to the larger total mass the tidal grinding duration for neutron star-black hole binaries is somewhat shorter than the above estimate, but for the low mass black holes that are most interesting for GRBs, e.g., Rosswog (2005), the difference is just a factor of two.

Naively, one would expect the major flaring activity to occur coincident with the first crust cracking (Equation (4)), and just by analogy with magnetar giant flares (Palmer et al. 2005), such precursors should have spectral properties similar to the properties of the main burst. The elastic energy stored within the deformed neutron star crust is $\sim 10^{46}\,(\sigma_{\rm max}/0.1)^2$ erg (Thompson 2001), and if this is the main energy source, the corresponding precursors would not be visible beyond 40–80 Mpc.

4.1.3. A Relativistic Jet Ploughing through a Pre-ejected, Neutrino-driven Baryonic Wind

Directly after the merger—but possibly before a relativistic jet can be launched—the remnant of a neutron star merger consists of a hot, differentially rotating, super-massive neutron star, surrounded by a massive ($\sim 0.1\ M_\odot$), thick accretion disk of neutron-rich debris (e.g., Ruffert & Janka 2001; Rosswog et al. 2003). In the inner parts of this disk, at a distance r from the center of the central object, a nucleon is gravitationally bound with an energy of $E_{\rm grav} \approx 35\ \mathrm{MeV}(\frac{M_{\rm co}}{2.5\,M_\odot})(\frac{100\,\mathrm{km}}{r})$. On the other hand, a large fraction of gravitational binding energy of the binary system is released in the form of neutrinos, with average energies of $\langle E_{\nu_e}\rangle \approx 10$ MeV, $\langle E_{\bar{\nu}_e}\rangle \approx 15$ MeV and $\langle E_{\nu_X}\rangle \approx 20$ MeV (Ruffert & Janka 2001; Rosswog & Liebendörfer 2003), where the index X refers collectively to the heavy lepton neutrinos. It had been realized early on (Ruffert et al. 1997; Rosswog & Ramirez-Ruiz 2002) that such a configuration should ablate a substantial fraction of the debris in a neutrino-driven, baryonic wind. A quantitative calculation beyond order of magnitude estimates has only recently become possible (Dessart et al. 2009). This study found that a bi-polar, non-relativistic ($v \sim 0.1c$) wind of $\dot{M} \sim 10^{-3}\ M_\odot\ \mathrm{s^{-1}}$ heavily pollutes the polar regions and prevents the formation of ultra-relativistic outflow. Thus, for at least as long as the central object has not collapsed into a black hole, it seems impossible to produce a GRB.

After a (likely, but not necessarily guaranteed) collapse, one is left with the "standard" central engine, a black hole–disk system. Once this happens, the neutrino-driven mass loss will be seriously reduced and jet formation seems likely. It may be speculated that the emerging relativistic jet has to plough through the pre-ejected neutrino-driven baryonic cloud, possibly producing a precursor signal. The details of such a jet–cloud interaction are very likely rather involved and a quantitative investigation of this issue is beyond the scope of this paper. We note however that as in this case the precursor marks the start of the central engine activity, the merging process could happen significantly before the observed main burst, stretching the temporal window over which a gravitational waves signal must be searched (Abadie et al. 2010).

4.2. Constraints on Quantum Gravity

GRB 090510 is accompanied by high-energy (>100 MeV) emission, lasting up to 200 s after the burst (Giuliani et al. 2010; De Pasquale et al. 2010). The detection of very energetic photons (up to 31 GeV) during the main prompt emission and

the high redshift of the source ($z = 0.903$; McBreen et al. 2010) led to very tight constraints on the quantum gravity mass M_{QG}, excluding a possible linear energy dependence of the propagation speed of light (Abdo et al. 2009). The authors adopt two different approaches to constrain Lorentz invariance violation effects: the former, based on the method outlined in Scargle et al. (2008), derives a limit on the quantum gravity mass of $M_{QG} > 1.22\ M_{Pl}$, where $M_{Pl} = 1.2 \times 10^{19}$ GeV c^{-2} is the Planck mass. This limit remains unchanged by the present findings.

As the photon emission time and location are unknown, the latter approach conservatively assumes that the observed 31 GeV photon has not been emitted before the onset of the low energy emission. Under this assumption, the limit on the quantum gravity mass is $M_{QG} > 1.19\ M_{Pl}$. In their calculation Abdo et al. (2009) considered the precursor at $T_0-0.5$ s, also detected by the *Fermi*/GBM (see Figure 1), as the earliest possible emission time. The detection of an earlier precursor, presented in this work, shows that emission started well before the GRB, implying a maximum delay of ∼13.3 s between the lowest and highest energy photons. The corresponding upper limit on the quantum gravity mass is therefore significantly reduced to $M_{QG} > 0.09\ M_{Pl}$.

5. CONCLUSION

We carried out a systematic search of precursors on the sample of short GRBs observed by *Swift*. We found that ∼8%–10% of short GRBs shows such early episode of emission, preceding the main GRB by a few seconds ($\Delta T \leqslant 13$ s). In our sample we found some evidence, though not yet conclusive, that the observed delay can be as long as ∼100 s. The spectral properties of these precursors do not substantially differ from the prompt emission. This result however might be partially a consequence of the *Swift*/BAT narrow bandpass.

We consider it unlikely that the observed precursors are produced by fireballs becoming optically thin, and argue instead that the preburst activity in short GRBs is related to their progenitors, i.e., compact objects mergers. We discuss three possible central engine-related mechanisms: the interaction of neutron star magnetospheres (Hansen & Lyutikov 2001), which requires one of the two compact objects to be a magnetar; flares from neutron star crust cracking, which predicts very long delays between the precursor and the main burst; and finally, analogously to long GRB precursors which are associated with the interaction of the relativistic jet with the stellar envelope, the precursors in short GRBs might be produced by the jet interacting with a pre-ejected neutrino-driven baryonic wind. In this last case, the precursor is produced after the merger and marks the start of the central engine activity.

We thank G. Skinner and C. Markwardt for discussions and useful suggestions on the *Swift*/BAT data analysis. This research was supported by an appointment to the NASA Postdoctoral Program at the Goddard Space Flight Center, administered by Oak Ridge Associated Universities through a contract with NASA.

REFERENCES

Abadie, J., et al. 2010, ApJ, 715, 1453
Abdo, A. A., et al. 2009, Nature, 462, 331
Abramowicz, M. A., Novikov, I. D., & Paczynski, B. 1991, ApJ, 369, 175
Ackermann, M., et al. 2010, ApJ, 716, 1178
Belczynski, K., Kalogera, V., & Bulik, T. 2002, ApJ, 572, 407
Belczynski, K., et al. 2006, ApJ, 648, 1110
Blinnikov, S. I., Novikov, I. D., Perevodchikova, T. V., & Polnarev, A. G. 1984, SvA, 10, L177
Bloom, J. S., Butler, N. R., & Perley, D. A. 2008, in AIP Conf. Ser. 1000, Gamma-ray Bursts 2007, ed. M. Galassi, D. Palmer, & E. Fenimore (New York: AIP), 11
Burlon, D., Ghirlanda, G., Ghisellini, G., Greiner, J., & Celotti, A. 2009, A&A, 505, 569
Burlon, D., et al. 2008, ApJ, 685, L19
Daigne, F., & Mochkovitch, R. 2002, MNRAS, 336, 1271
De Pasquale, M., et al. 2010, ApJ, 709, L146
Dessart, L., Ott, C. D., Burrows, A., Rosswog, S., & Livne, E. 2009, ApJ, 690, 1681
Eichler, D., Livio, M., Piran, T., & Schramm, D. N. 1989, Nature, 340, 126
Giuliani, A., et al. 2010, ApJ, 708, L84
Goodman, J. 1986, ApJ, 308, L47
Hansen, B. M. S., & Lyutikov, M. 2001, MNRAS, 322, 695
Harding, A. K., & Lai, D. 2006, Rep. Prog. Phys., 69, 2631
Heyl, J. S., & Kulkarni, S. R. 1998, ApJ, 506, L61
Horowitz, C. J., & Kadau, K. 2009, Phys. Rev. Lett., 102, 191102
Hurley, K., et al. 2005, Nature, 434, 1098
Koshut, T. M., et al. 1995, ApJ, 452, 145
Lazzati, D. 2005, MNRAS, 357, 722
Lazzati, D., & Begelman, M. C. 2005, ApJ, 629, 903
Lazzati, D., Campana, S., Rosati, P., Panzera, M. R., & Tagliaferri, G. 1999, ApJ, 524, 414
Lyutikov, M., & Blandford, R. 2003, arXiv:astro-ph/0312347
Lyutikov, M., & Usov, V. V. 2000, ApJ, 543, L129
McBreen, S., et al. 2008, ApJ, 677, L85
McBreen, S., et al. 2010, A&A, 516, A71
Mészáros, P., Ramirez-Ruiz, E., & Rees, M. J. 2001, ApJ, 554, 660
Metzger, B. D., Quataert, E., & Thompson, T. A. 2008, MNRAS, 385, 1455
Morsony, B. J., Lazzati, D., & Begelman, M. C. 2007, ApJ, 665, 569
Murakami, T., Inoue, H., Nishimura, J., van Paradijs, J., & Fenimore, E. E. 1991, Nature, 350, 592
Nakamura, T. 2000, ApJ, 534, L159
Narayan, R., Paczynski, B., & Piran, T. 1992, ApJ, 395, L83
Norris, J. P., & Bonnell, J. T. 2006, ApJ, 643, 266
Owen, B. J. 2005, Phys. Rev. Lett., 95, 211101
Paciesas, W. S., et al. 1999, ApJS, 122, 465
Paczynski, B. 1986, ApJ, 308, L43
Paczynski, B. 1991, Acta Astron., 41, 257
Page, K. L., et al. 2007, ApJ, 663, 1125
Palmer, D. M., et al. 2005, Nature, 434, 1107
Peters, P. C. 1964, Phys. Rev., 136, 1224
Piran, T. 1999, Phys. Rep., 314, 575
Piro, L., et al. 2005, ApJ, 623, 314
Ramirez-Ruiz, E., Celotti, A., & Rees, M. J. 2002, MNRAS, 337, 1349
Ramirez-Ruiz, E., Merloni, A., & Rees, M. J. 2001, MNRAS, 324, 1147
Rees, M. J., & Meszaros, P. 1994, ApJ, 430, L93
Rizzuto, D., et al. 2007, MNRAS, 379, 619
Rosswog, S. 2005, ApJ, 634, 1202
Rosswog, S., & Liebendörfer, M. 2003, MNRAS, 342, 673
Rosswog, S., & Ramirez-Ruiz, E. 2002, MNRAS, 336, L7
Rosswog, S., Ramirez-Ruiz, E., & Davies, M. B. 2003, MNRAS, 345, 1077
Ruffert, M., & Janka, H. 2001, A&A, 380, 544
Ruffert, M., Janka, H., Takahashi, K., & Schaefer, G. 1997, A&A, 319, 122
Ruffini, R., et al. 2008, in AIP Conf. Ser. 1065, The Canonical Gamma-Ray Bursts and Their "Precursors", ed. Y.-F. Huang, Z.-G. Dai, & B. Zhang (New York: AIP), 219
Scargle, J. D., Norris, J. P., & Bonnell, J. T. 2008, ApJ, 673, 972
Thompson, C. 2001, in Proc. NATO Advanced Study Institute 567, The Neutron Star–Black Hole Connection, ed. C. Kouveliotou, J. Ventura, & E. van den Heuvel (Dordrecht: Kluwer), 369
Thompson, C., & Duncan, R. C. 1995, MNRAS, 275, 255
Torrence, C., & Compo, G. P. 1998, Bull. Am. Meteorol. Soc., 79, 61
Troja, E., King, A. R., O'Brien, P. T., Lyons, N., & Cusumano, G. 2008, MNRAS, 385, L10
Umeda, H., Tominaga, N., Maeda, K., & Nomoto, K. 2005, ApJ, 633, L17
Ushomirsky, G., Cutler, C., & Bildsten, L. 2000, MNRAS, 319, 902
Vanderspek, R., et al. 2004, ApJ, 617, 1251
Wang, X., & Mészáros, P. 2007, ApJ, 670, 1247
Waxman, E., & Mészáros, P. 2003, ApJ, 584, 390
Zhang, W., Woosley, S. E., & MacFadyen, A. I. 2003, ApJ, 586, 356
Zhang, B., et al. 2009, ApJ, 703, 1696